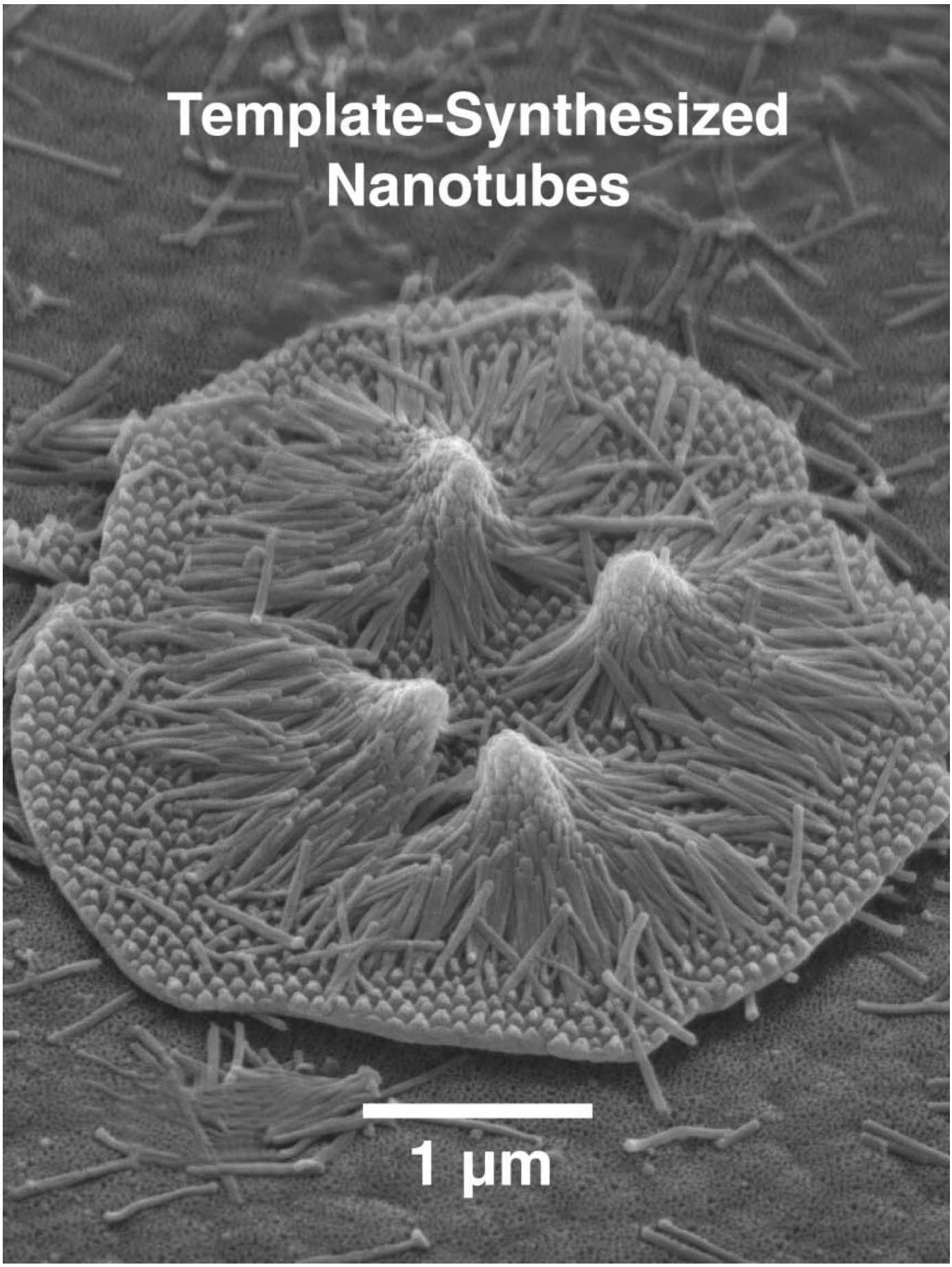

0947-6539/02/0816-3572 $ 17.50+.50/0 *Chem. Eur. J.* **2002**, *8*, No. 16

Template-Synthesized Nanotubes for Chemical Separations and Analysis

Marc Wirtz,[a] Matthew Parker,[a] Yoshio Kobayashi,[b] and Charles R. Martin*[a]

Abstract: We have developed a new class of synthetic membranes that consist of a porous polymeric support that contains an ensemble of gold nanotubes that span the thickness of the support membrane. The support is a commercially-available microporous polycarbonate filter with cylindrical nanoscopic pores. The gold nanotubes are prepared by electroless deposition of Au onto the pore walls, that is, the pores acts as templates for the nanotubes. We have shown that by controlling the Au deposition time, Au nanotubes that have effective inside diameters of molecular dimensions (<1 nm) can be prepared. These nanotube membranes can be used to cleanly separate small molecules on the basis of molecular size. Furthermore, use of these membranes as a novel electrochemical sensor is also discussed. This new sensing scheme involves applying a constant potential across the Au nanotube membrane and measuring the drop in the transmembrane current upon the addition of the analyte. This paper reviews our recent progress on size-based based transport selectivity and sensor applications in this new class of membranes.

Keywords: molecular sieving · nanotechnology · sensors · template synthesis

Introduction

We have been investigating a general method for preparing nanomaterials called template synthesis.[1–3] This method entails synthesis or deposition of the desired material within the cylindrical and monodisperse pores of a nanopore membrane or other solid. We have used polycarbonate filters, prepared by the track-etch method,[4] and nanopore aluminas, prepared electrochemically from Al foil,[5] as our template materials. Cylindrical nanostructures with monodisperse diameters and lengths are obtained, and depending on the membrane and synthetic method used, these may be solid nanowires or hollow nanotubes. We, and others, have used this method to prepare nanowires and tubes composed of metals,[5–15] polymers,[16–19] semiconductors,[20, 21] carbons,[22–24] and Li^+ intercalation materials.[25–27] It is also possible to prepare composite nanostructures, both concentric tubular composites, where an outer tube of one material surrounds an inner tube of another,[28, 29] and segmented composite nanowires.[30]

One of our earliest applications of the template method was to prepare ensembles of microscopic and nanoscopic electrodes.[31–34] Such electrodes are prepared by depositing noble metals within the pores of the polycarbonate filtration membranes. Initially, we deposited the metal in the pores using electrochemical-plating methods,[31] but we ultimately discovered that electroless plating allowed for more uniform metal deposition.[33] In the electroless method, metal deposition begins at the pore walls creating, at short deposition time, hollow metal nanotubes within the pores.[8–12, 35, 36] That is, the electroless plating method yields metal (typically gold) nanotube membranes, the subject of this review.

Membrane Preparation and Analysis

Template membranes, electroless plating and estimation of the nanotube inside diameter: Commercially available polycarbonate filters prepared using the track-etch method are used as the templates for the Au nanotube membranes. Filters with cylindrical 30 nm diameter pores, 6×10^8 pores per cm^2 of membrane surface area, are typically used.[8, 9, 37, 38] An electroless plating method is used to deposit the Au nanotubes within the pores (Figure 1A).[33] Briefly, a catalyst is first applied to all surfaces (membrane faces plus pore walls) of the membrane. The membrane is then immersed into the electroless plating bath which contains a Au^I species and a chemical reducing agent. Because the reduction of Au^I to metallic Au only occurs in the presence of the catalyst, Au nanotubes that line the pore walls (Figure 1B) (as well as Au surface films on both faces of the membrane) are obtained.[8–10, 37, 38]

[a] Prof. C. R. Martin, Dr. M. Wirtz, M. Parker
Department of Chemistry and Center for Research at the Bio/Nano Interface
University of Florida, Gainesville, FL 32611 (USA)
Fax: (+1) 352-392-8206
E-mail: crmartin@chem.ufl.edu

[b] Prof. Dr. Y. Kobayashi
Current address: Department of Chemical Engineering
Graduate School of Engineering, Tohoku University
Sendai 980-8579 (Japan)

  0947-6539/02/0816-3573 $ 17.50+.50/0

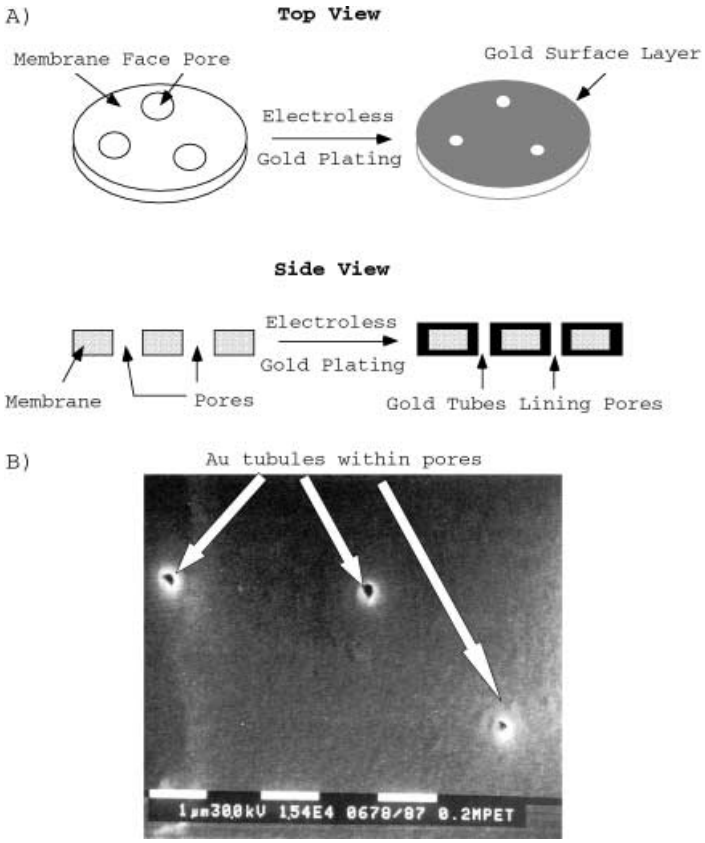

Figure 1. A) Schematic of the electroless plating process used to prepare that Au nanotube membranes. B) Scanning electron micrograph (SEM) of the surface of a polycarbonate template membrane showing three Au nanotubes deposited within the pores. To visualize the tubes by SEM, the membrane had larger pores than those used to prepare the nanotube membranes discussed here.

The thicknesses of both the Au surface films and nanotube walls increase with electroless plating time. As a result of the thickening of the nanotube walls, the inside diameter (id) of the tubes decreases with plating time. The id is measured using a gas transport method described previously.[8–11, 37–39] At long plating times, membranes containing nanotubes with ids of molecular dimensions are obtained (Figure 2). Finally, depending on the application, the Au surface films can be either left on the faces of the membrane or removed.

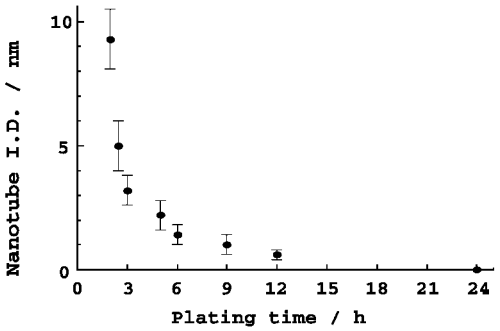

Figure 2. Variation of the nanotube effective inside diameter with plating time.

Transport Properties of the Au Nanotube Membranes

Molecular-sieving in single-molecule permeation experiments: These experiments were done in a simple U-tube permeation cell in which the nanotube membrane separates a feed half-cell from a permeate half-cell. The feed half-cell is charged with a solution of the molecule whose transport properties through the membrane are to be evaluated (often called the permeate molecule). The permeate half-cell is initially water or a salt solution. Passive diffusion transports the permeate molecule from the feed half-cell, through the nanotube membrane, and into the permeate half-cell. The permeate half-cell is periodically assayed to determine the time-dependence of transport of the permeate molecule through the membrane.

The transport data are processed as plots of moles of permeate transported versus time. Straight-line plots are obtained and the flux of the permeate molecule through the membrane is calculated from the slope. The experiment is then repeated using a solution of a second permeate molecule in the feed half-cell. A membrane-transport selectivity coefficient (α) can then be obtained by using the ratios of the fluxes for the two permeate molecules. Since molecular-sized based selectivity is of interest here, one of the permeate molecules was large—the tris-bipyridal complex of Ru^{II}, $[Ru(bpy)_3]^{2+}$—and the other was smaller—methyl viologen, MV^{2+} (Figure 3).

The ratio of the diffusion coefficients for MV^{2+} and $[Ru(bpy)_3]^{2+}$ in free aqueous solution is 1.5.[40, 41] For this reason, if a simple solution-like diffusion process were operative in the nanotubes, a selectivity coefficient of $\alpha = 1.5$ would be anticipated. In contrast, even for the largest id nanotubes investigated (5.5 nm), the selectivity coefficient was substantially greater, $\alpha = 50$ (Figure 4A). These data suggest that size-based molecular sieving occurs in these large-id (> molecular dimensions) nanotubes.[9, 42, 43] This is reflected in the transport data (Figure 4A) where the flux of the larger $[Ru(bpy)_3]^{2+}$ is decreased more than the flux for the smaller MV^{2+}. As a result $\alpha = 50$ is obtained. As the nanotube id is made smaller, the α value should become even larger, which is also reflected in the experimental transport data. Values for the 5.5 nm, 3.2 nm and 2.0 nm id nanotube membranes are $\alpha = 50$, 88, and 172, respectively.

Molecular filtration in two-component permeation experiments: The smallest id nanotube membrane investigated (id $\sim$0.6 nm) provides a measurable flux for MV^{2+}, but the larger $[Ru(bpy)_3]^{2+}$ could not be detected in the permeate solution, even after a two week permeation experiment (Figure 4B). These data suggest that clean separation (molecular filtration) of these two species should be possible with this nanotube membrane. This was proven by doing two-molecule permeation experiments, where both the larger and smaller molecules (Figure 3) were present in the feed half-cell together (see Table 1 for the large-molecule/small-molecule pairs investigated). For all three of the large-molecule/small-

  0947-6539/02/0816-3574 $ 17.50+.50/0 *Chem. Eur. J.* **2002**, *8*, No. 16

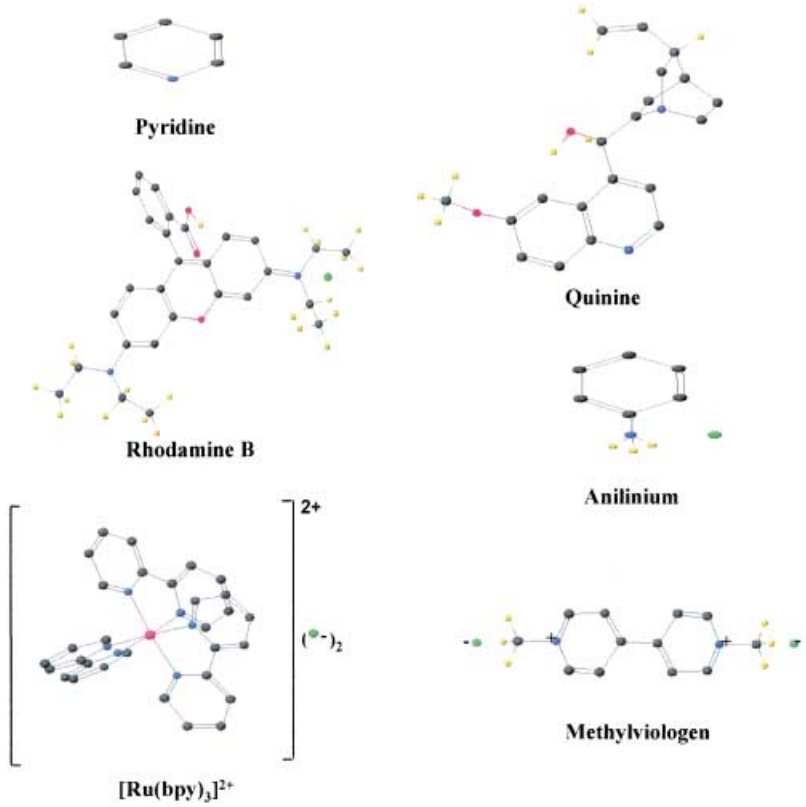

Figure 3. Chemical structures and approximate relative sizes of the three "big molecule/small molecule" pairs used in the molecular filtration experiments. Quinine, MV^{2+}, and $[Ru(bpy)_3]^{2+}$ were also used as analytes in the sensor work.

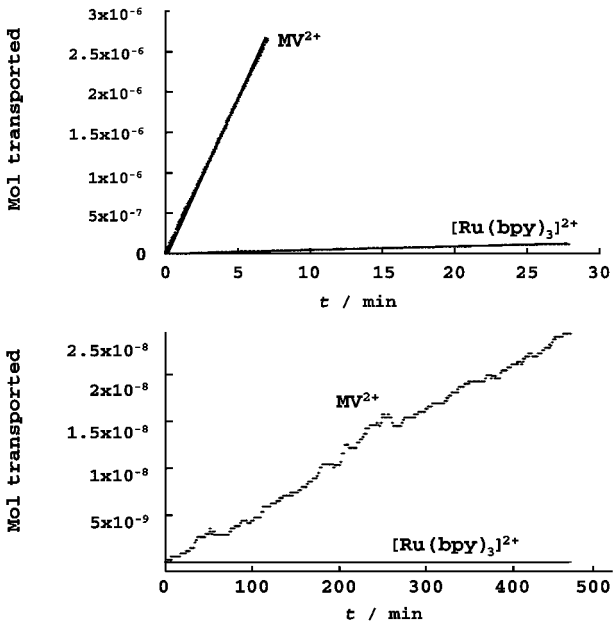

Figure 4. Single-molecule permeation experiments showing moles of MV^{2+} and $[Ru(bpy)_3]^{2+}$ transported versus time. Membranes contained nanotubes with ids of A) 5.5 nm, B) < 0.6 nm. Only MV^{2+} was transported through this membrane.

Table 1. Minimal membrane-transport selectivity coefficients.

Permeate pair	α_{min}
pyridine/quinine	15000
anilinium/rhodamine	130000
$MV^{2+}/[Ru(bpy)_3]^{2+}$	1500

molecule pairs shown in Figure 3, the small molecule could be easily detected in the permeate solution but the large molecule was undetectable.[9]

These data show that within the limits of the measurement, the Au nanotube membrane can cleanly separate large molecules from small molecules. However, one could argue that the large molecule is, indeed, present in the permeate solution but at a concentration just below the detection limit of the analytical method employed. This argument allows us to define a minimal transport selectivity coefficient (α_{min}) for each small-molecule/large-molecule pair investigated, where α_{min} is defined as the measured concentration of the small molecule in the permeate solution divided by the detection limit for the large molecule. The α_{min} values obtained are extraordinary (Table 1). It is important to stress again that, in all three cases, the larger molecule was undetectable in the permeate solution.

Chemical Sensing with the Au Nanotube Membranes

In addition to the above possible applications in size-based separations, these Au nanotube membranes have been used as sensors for the determination of ultratrace concentrations of ions and molecules.[37, 38, 45] In this case, the nanotube membrane was allowed to separate two salt solutions, a constant transmembrane potential was applied, and the resulting transmembrane current was measured. When an analyte of comparable dimensions to the inside diameter of the nanotubes was added to one of the salt solutions, a decrease in transmembrane current is observed. The magnitude of this drop in transmembrane current (Δi) is proportional to the analyte concentration.

Calibration curves and detection limits: As in the transport experiments, a U-tube cell was assembled with the nanotube membrane separating the two halves of the cell. The experimental protocol used with these cells was to immerse the electrodes into the appropriate electrolyte and apply a constant potential between the electrodes. Three different sets of electrodes and electrolytes were used. The first set consisted of two Pt plate electrodes, and the electrolyte used in both half-cells was 0.1M KF. The second set consisted of two

Ag/AgCl wires, and the electrolyte used in both half-cells was 0.1M KCl. The third set consisted of two Ag/AgI wires immersed in 0.1M KI. The resulting transmembrane current was measured and recorded on an *X-t* recorder. After obtaining this baseline current, the anode half-cell was spiked with a known quantity of the desired analyte (Figure 3). This resulted in a change in the transmembrane current, Δi (Figure 5). A potentiostat was used to apply the potential between the electrodes and measure the transmembrane current. The transmembrane potential used was on the order of 0.5 V.[38]

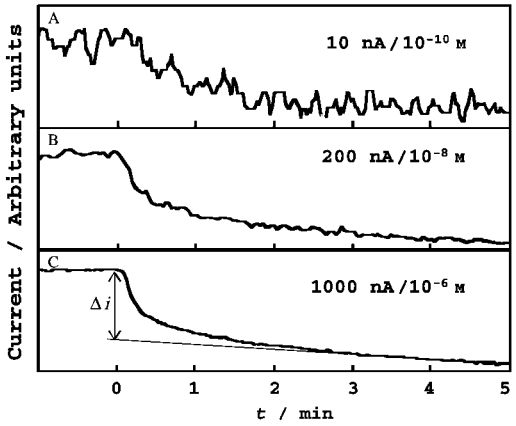

Figure 5. Nanotube membrane sensor current-time transients associated with spiking the anode half cell with the indicated concentrations of $[Ru(bpy)_3]^{2+}$. Tube id = 2.8 nm; Ag/AgCl/KCl cell Δi determined as shown in C.

Plots of $\log\Delta i$ versus log[analyte] for the analytes $[Ru(bpy)_3]^{2+}$, MV^{2+} and quinine (Figure 3) were obtained using Ag/AgCl electrodes and 0.1M KCl as the electrolyte in both half-cells (Figure 6). A membrane with 2.8 nm id Au nanotubes was used. A log/log format is used for these

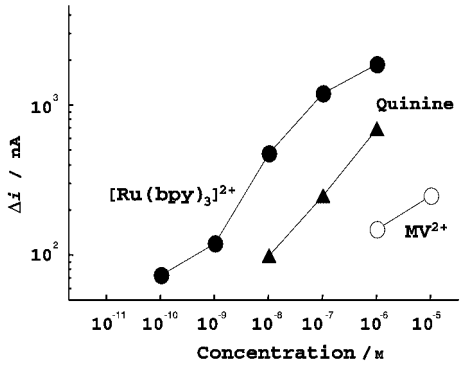

Figure 6. Calibrations curves for the indicated analytes. Membrane and cell as per Figure 5.

"calibration curves" because of the large dynamic range (spanning as much as five orders of magnitude in analyte concentration) obtained with this cell. Analogous calibration curves were obtained for the other electrode/electrolyte systems investigated. The detection limits obtained are shown in Table 2.[38] For the divalent cationic electrolytes, the detection limits were lowest (best) in the Ag/AgI/KI cell and worst in the Pt/KF cell. The detection limit for quinine was the same in both the Ag/AgI/KI and Ag/AgCl/KCl cells. In general, the detection limit decreases as the size of the analyte molecule increases (see Figure 6). Finally, the detection limits obtained (down to 10^{-11}M) are extraordinary and compete with even the most sensitive of modern analytical methods.

Table 2. Detection limits obtained for the three different electrode/electrolyte systems studied.[a]

Electrode	Electrolyte	Concentration [M]
Pt/KF	$[Ru(bpy)_3]^{2+}$	10^{-9}
Ag/AgCl/KCl	$[Ru(bpy)_3]^{2+}$	10^{-10}
	quinine	10^{-8}
	MV^{2+}	10^{-6}
	2-naphthol	10^{-6}
Ag/AgI/KI	$[Ru(bpy)_3]^{2+}$	10^{-11}
	quinine	10^{-8}
	MV^{2+}	10^{-7}
	2-naphthol	10^{-6}

[a] Nanotube id = 2.8 nm.

The majority of the quinine in both the KCl and KI solutions is present as the monoprotonated (monocationic) form. Perhaps the reason the detection limits for $[Ru(bpy)_3]^{2+}$ and MV^{2+} are lower in the Ag/AgI/KI cell while the detection limit for quinine is the same in both this cell and the Ag/AgCl/KCl cell has to do with the difference in charge of these analytes (predominately monocationic versus dicationic). To explore this point, the detection limits for a neutral analyte, 2-naphthol, were obtained in both the Ag/AgI/KI and Ag/AgCl/KCl cells. Like quinine, the detection limit for this neutral analyte was the same in both cells (10^{-6}M, Table 2).

In the membrane transport studies it was shown that $[Ru(bpy)_3]^{2+}$ and MV^{2+} come across such membranes as the ion multiples $[Ru(bpy)_3]^{2+}(X^-)_2$ and $MV^{2+}(X^-)_2$ (X^- = anion).[9] In the KI cell, the ion multiple contains two larger (relative to chloride) iodide anions. Perhaps the larger size of the iodide ion multiple accounts for the lower detection limit in the KI-containing cell. If this is true then the difference between the quinine cation paired with one I^- versus this cation paired with one Cl^- is not great enough to cause the detection limit for this predominately monovalent analyte to be significantly different in the Ag/AgI/KI versus the Ag/AgCl/KCl cells (Table 2).

The final variable to be investigated is the effect of nanotube inside diameter on detection limit. To explore this parameter, membranes with nanotube ids of approximately of 3.8, 2.8, 2.2, 1.8, and 1.4 nm were prepared and used in the Ag/AgI/KI cell.[38] Calibration curves for the analytes $[Ru(bpy)_3]^{2+}$, MV^{2+} and quinine were generated as before, and detection limits were obtained from these calibration curves. Figure 7 shows plots of detection limit for these three different analytes versus the nanotube id in the membrane used. A minimum in this plot is observed for each of the three analytes.

The nanotube membrane that produces this minimum (best) detection limit depends on the size of the analyte. These molecules decrease in size in the order $[Ru(bpy)_3]^{2+}$ >

  0947-6539/02/0816-3576 $ 17.50+.50/0 *Chem. Eur. J.* **2002**, *8*, No. 16

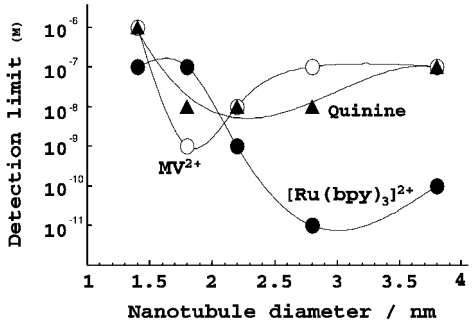

Figure 7. Detection limits for MV^{2+}, quinine, and $[Ru(bpy)_3]^{2+}$ versus id of the nanotubes used in the sensor.

quinine > MV^{2+} (Figure 7). The nanotube membrane that yields the lowest detection limit follows this size order, that is, the nanotube diameters that produce the lowest detection limit for $[Ru(bpy)_3]^{2+}$, quinine, and MV^{2+} are 2.8 nm, 2.2 nm, and 1.8 nm, respectively. For the roughly spherical analytes, the optimal tube diameter is a little over twice the diameter of the molecule.

Molecular-size-based selectivity: The data presented so far show a strong correlation between detection limit and the relative sizes of the nanotube and the analyte molecule (Figure 3). This indicates that this device should show molecular-size-based selectivity. This is not surprising given the transport studies discussed above. To explore size-based selectivity, a series of solutions was prepared containing decreasing concentrations of the analyte species, but containing a constant (higher) concentration of an interfering species. The interfering species was smaller than the analyte species. The response of a 2.8 nm nanotube membrane to these solutions was then measured starting from lowest to highest concentration of the analyte species in the Ag/AgI/KI cell.

The small pyridine molecule was used as an interfering species. When present at a concentration of 10^{-4} M, pyridine offered very little interference for any of the analytes $[Ru(bpy)_3]^{2+}$, MV^{2+} or quinine. The detection limits in the presence of 10^{-4} M pyridine were 10^{-10} M for $[Ru(bpy)_3]^{2+}$, 10^{-6} M for MV^{2+} and 10^{-7} M for quinine, within an order of magnitude of the detection limit with no added interfering species (Table 2). Put another way, this nanotube-membrane sensor can detect 10^{-10} M $[Ru(bpy)_3]^{2+}$ in the presence of six orders of magnitude higher pyridine concentration. These experiments show that, in agreement with the transport studies, the nanotube membrane-based sensor can show excellent size-based selectivity.

Conclusion

In this review, we have focused on using the Au nanotube membranes to separate small molecules on the basis of size. We have shown here that these membranes can act as extraordinary molecular sieves. In addition, we have described a new and highly sensitive approach to electroanalysis based on the Au nanotube membranes. This method involves applying a constant potential across the membrane and measuring the drop in the trans-membrane current upon the addition of the analyte. Detection limits as low as 10^{-11} M were obtained. Previous studies have demonstrated that these Au nanotube membranes can show ionic charge-based transport selectivity and that the membranes can be electrochemically switched between anion transporting and cation transporting states.[8] Hence, these membranes can be viewed as universal ion exchangers. Furthermore, chemical transport selectivity can be introduced into these membranes by chemisorbing thiols to the inside tube walls.[10, 11] Hence, these nanotube membranes can utilize all of the selectivity paradigms (sterics, electrostatics, and chemical interactions) that Mother Nature uses in the design of Her exquisitely selective molecular-recognition schemes. Such research at the bio/nano interface is of great current interest in our group.

Acknowledgements

Aspects of this work were funded by the National Science Foundation, the Office of Naval Research and the Department of Energy.

[1] C. R. Martin, *Science* **1994**, *266*, 1961–1966.
[2] J. C. Hulteen, C. R. Martin, *J. Mater. Chem*. **1997**, *7*, 1075–1087.
[3] C. R. Martin, D. T. Mitchell, *Anal. Chem*. **1998**, *70*, 322A–327A.
[4] R. L. Fleischer, P. B. Price, R. M. Walker, *Nuclear Tracks in Solids*, University of California Press, Berkeley, **1975**.
[5] G. L. Hornyak, C. J. Patrissi, C. R. Martin, *J. Phys. Chem. B* **1997**, *101*, 1548–1555.
[6] G. E. Possin, *Rev. Sci. Instrum*. **1970**, *41*, 772–774.
[7] W. D. Williams, N. Giordano, *Rev. Sci. Instrum*. **1984**, *55*, 410–412.
[8] M. Nishizawa, V. P. Menon, C. R. Martin, *Science* **1995**, *268*, 700–702.
[9] K. B. Jirage, J. C. Hulteen, C. R. Martin, *Science* **1997**, *278*, 655–658.
[10] J. C. Hulteen, K. B. Jirage, C. R. Martin, *J. Am. Chem. Soc.* **1998**, *120*, 6603–6604.
[11] K. B. Jirage, J. C. Hulteen, C. R. Martin, *Anal. Chem.* **1999**, *71*, 4913–4918.
[12] Z. Hou, N. L. Abbott, P. Stroeve, *Langmuir* **2000**, *16*, 2401–2404.
[13] G. Tourillon, L. Pontinnier, J. P. Levy, V. Langlais, *Electrochem. Solid-State Lett.* **2000**, *3*, 20–23.
[14] C. Schonenberger, B. M. I. van der Zande, L. G. J. Fokkink, M. Henry, C. Schmid, M. Kruger, A. Bachtold, R. Huber, H. Birk, U. Staufer, *J. Phys. Chem. B* **1997**, *101*, 5497–5505.
[15] C. K. Preston, M. J. Moskovits, *J. Phys. Chem.* **1993**, *97*, 8495–8503.
[16] C. R. Martin in *Handbook of Conducting Polymers* (Eds.: J. R. Reynolds, T. Skotheim, R. Elsebaumer), 2nd ed., Marcel Dekker, **1997**, pp. 409–421.
[17] J. Duchet, R. Legras, S. Demoustier-Champagne, *Synth. Met.* **1998**, *98*, 113–122.
[18] S. Demoustier-Champagne, P.-Y. Stavaux, *Chem. Mater.* **1999**, *11*, 829–834.
[19] S. Sukeerthi, Q. Contractor, *Anal. Chem.* **1999**, *71*, 2231–2236.
[20] B. B. Lakshmi, C. J. Patrissi, C. R. Martin, *Chem. Mater*. **1997**, *9*, 2544–2550.
[21] B. B. Lakshmi, P. K. Dorhout, C. R. Martin, *Chem. Mater.* **1997**, *9*, 857–862.
[22] G. Che, B. B. Lakshmi, C. R. Martin, E. R. Fisher, *Langmuir* **1999**, *15*, 750–758.
[23] G. Che, E. R. Fisher, C. R. Martin, *Nature* **1998**, *393*, 346–349.
[24] T. Kyotani, L. F. Tsai, A. Tomita, *Chem. Commun*. **1997**, *701*.
[25] C. J. Patrissi, C. R. Martin, *J. Electrochem. Soc*. **1999**, *146*, 3176–3180.
[26] N. Li, C. J. Patrissi, C. R. Martin, *J. Electrochem. Soc.* **2000**, *147*, 2044–2049.
[27] G. Che, K. B. Jirage, E. R. Fisher, C. R. Martin, H. Yoneyama, *J. Electrochem. Soc.* **1997**, *144*, 4296–4302.

[28] V. M. Cepak, J. C. Hulteen, G. Che, K. B. Jirage, B. B. Lakshmi, E. R. Fisher, C. R. Martin, *J. Mater. Res.* **1998**, *13*, 3070 – 3080.
[29] V. M. Cepak, J. C. Hulteen, G. Che, K. B. Jirage, B. B. Lakshmi, E. R. Fisher, C. R. Martin, *Chem. Mater.* **1997**, *9*, 1065 – 1067.
[30] B. R. Martin, D. J. Dermody, B. D. Reiss, M. Fang, L. A. Lyon, M. J. Natan, T. E. Mallouk, *Adv. Mater.* **1999**, *11*, 1021 – 1025.
[31] R. M. Penner, C. R. Martin, *Anal. Chem.* **1987**, *59*, 2625 – 2530.
[32] I. F. Cheng, C. R. Martin, *Anal. Chem*. **1988**, *60*, 2163 – 2165.
[33] V. P. Menon, C. R. Martin, *Anal. Chem.* **1995**, *67*, 1920 – 1928.
[34] J. C. Hulteen, V. P. Menon, C. R. Martin, *J. Chem. Soc. Faraday Trans. 1* **1996**, *92*, 4029 – 4032.
[35] M. S. Kang, C. R. Martin, *Langmuir* **2001**, *17*, 2753 – 2759.
[36] S. B. Lee, C. R. Martin, *Anal.Chem*. **2001**, *73*, 768 – 775.
[37] Y. Kobayashi, C. R. Martin, *Anal. Chem.* **1999**, *71*, 3665 – 3672.
[38] Y. Kobayashi, C. R. Martin, *J. Electroanal. Chem.* **1997**, *431*, 29 – 33.
[39] W. J. Petzny, J. A. Quinn, *Science* **1969**, *166*, 751 – 753.
[40] Z. Prat, Y.-M. Tricot, I. Rubinstein, *J. Electroanal. Chem*. **1991**, *315*, 225 – 243.
[41] C. R. Martin, I. Rubinstein, A. J. Bard, *J. Electroanal. Chem*. **1983**, *115*, 267 – 271.
[42] V. M. Deen, *AICHEJ* **1987**, *33*, 1409 – 1425.
[43] I. A. Kathawalla, J. L. Anderson, J. S. Lindsey, *Macromolecules* **1989**, *22*, 1215 – 1219.
[44] T. K. Rostovtseva, *J. Membr. Biol*. **1996**, *151*, 29.
[45] H. Bayley, C. R. Martin, *Chem. Rev.* **2000**, *100*, 2575 – 2594.

  0947-6539/02/0816-3578 $ 17.50+.50/0